Reeves, et al., J. Geophys. Res., 98, 21,323, 1993.

Structured Plasma Sheet Thinning Observed by Galileo and 1984-129

G. D. Reeves[1], R. D. Belian[1], T. A. Fritz[1], M. G. Kivelson[3], R. W. McEntire[2]
E. C. Roelof[2], B. Wilken[4], and D. J. Williams[2]

On December 8, 1990, the Galileo spacecraft used the Earth for a gravity assist on its way to Jupiter. Its trajectory was such that it crossed geosynchronous orbit at approximately local midnight between 1900 and 2000 UT. At the same time, spacecraft 1984-129 was also located at geosynchronous orbit near local midnight. Several flux dropout events were observed when the two spacecraft were in the near-Earth plasma sheet in the same local time sector. Flux dropout events are associated with plasma sheet thinning in the near-Earth tail during the growth phase of substorms. This period is unique in that Galileo provided a rapid radial profile of the near-Earth plasma sheet while 1984-129 provided an azimuthal profile. With measurements from these two spacecraft we can distinguish between spatial structures and temporal changes. Our observations confirm that the geosynchronous flux dropout events are consistent with plasma sheet thinning which changes the spacecraft's magnetic connection from the trapping region to the more distant plasma sheet. However, for this period, thinning occurred on two spatial and temporal scales. The geosynchronous dropouts were highly localized phenomena of ≈30 min duration superimposed on a more global reconfiguration of the tail lasting approximately 4 hours.

Background

The primary mission of the Galileo spacecraft is the investigation of the magnetosphere and atmosphere of Jupiter. However, two Earth flyby gravity assists provide opportunities to apply Galileo's instruments to the investigation of the Terrestrial magnetosphere. The "Galileo Earth-1" flyby took place on December 8, 1990. Galileo's trajectory is shown in Figure 1. Galileo entered the Earth's magnetosphere in the distant tail, rapidly flew toward the Earth, crossed geosynchronous orbit near local midnight, passed the Earth, and exited the magnetosphere in the prenoon sector. Figures 2 and 3 show the trajectories of Galileo and geosynchronous spacecraft 1984-129 during the period of closest approach, between 1700 and 2000 UT. Figure 2 is a local time plot which shows that Galileo came from the tail toward the Earth while 1984-129 made an azimuthal pass through local midnight at geosynchronous orbit. The universal time (in hours) for each spacecraft is given next to the large dots. Galileo crossed geosynchronous orbit shortly after 1900 UT when 1984-129 was at nearly the same local time. Figure 3 shows the trajectories as a function of Z-GSM and radius. In these coordinates the geosynchronous spacecraft 1984-129 remains essentially motionless. Also shown are the field line traces through 1984-129 according to the *Tsyganenko* [1989] field model for three levels of activity, Kp = 0, 2, and >4+ (which is its most stretched configuration). We see that 1984-129 and Galileo were on opposite sides of the magnetic equator and that both were nearly equidistant from the model magnetic equatorial plane. (Exact symmetry would be obtained at the point in the northern hemisphere where the three field line traces for various Kp intersect.)

This unique conjunction of spacecraft allows us to examine the radial and azimuthal profiles of the inner edge of the plasma sheet simultaneously. Such observations would be interesting under any circumstances. But, as we shall see below, the conjunction took place during a series of flux dropout events. Flux dropout events are commonly observed at geosynchronous orbit [*Lezniak and Winckler,* 1970; *Bogott and Mozer*, 1974; *Walker et al.,* 1978; *Baker et al.,* 1979; *Belian et al.,* 1981]. The term refers to the near disappearance of energetic particle fluxes measured by a satellite detector. Typically, over a period of approximately one half hour, fluxes of particles with energies greater than several tens of keV will decrease from their normal levels to near or below the detection threshold. Electron and proton fluxes usually decrease simultaneously. Energetic particle flux dropouts may be observed on the dayside as a result of magnetopause crossings but they are more typically observed near local midnight in association with the growth phase of a substorm [*Sauvaud and Winckler*, 1980].

The standard interpretation of flux dropout events is that they are a consequence of thinning of the near-Earth plasma sheet (where the "near-Earth plasma sheet" includes the outer trapping and quasi-trapping regions) [*Hones et al.,* 1967, 1973; *Baker et al.,* 1981; *Baker and McPherron,* 1990; *Lui,* 1991]. The changes which produce dropouts are illustrated schematically in Figure 4. The three field lines drawn show the rotation of the local field and the changing magnetic connection produced as the plasma sheet thins from a dipolelike configuration to a taillike one. The shaded band in Figure 4 represents a gradient of the energetic particle fluxes with darker shading representing higher fluxes although, in reality, the gradient is expected to be steepest in the trapping boundary rather than smooth as drawn. During the growth phase of a substorm the cross-tail current intensifies. This additional current distorts the field lines such that they appear more compressed in the *Z direction* or more stretched in the X direction. As a consequence, a spacecraft which is not on the magnetic equator becomes magnetically connected to points increasingly further downtail. As the spacecraft becomes magnetically connected to weaker and weaker fluxes of energetic particles, a flux dropout is observed. When there is a gradient in the fluxes of both protons and electrons, a dropout will be observed in both the proton and electron measurements. When the field dipolarizes, the fluxes return to their previous levels. If there has been any energization of the particles, then fluxes return to a higher level, and the event is termed a su bstorm injection [e.g., *Arnoldy and Chan,* 1969; *McIlwain,* 1974].

Although flux dropouts have been studied extensively, it is exceptional to have two spacecraft simultaneously on the midnight meridian in positions where the phenomenon should be observable. The fortuitous two spacecraft observations reported here allowed us to differentiate between spatial structures and temporal changes and revealed some unexpected features.

Observations

Instruments

Spacecraft 1984-129 was one of a continuously operating constellation of three geosynchronous spacecraft that carried Los Alamos charged particle analyzer (CPA) instruments from 1976 to the present. The CPA includes two instrument subsystems for measuring "low-energy" electrons (LoE) and "low-energy" protons (LoP). The LoE sub-system consists of five telescopes that measure electrons in six nested energy channels. The low-energy thresholds of those six channels are 30, 45, 65, 95, 140, and 200 keV. All share a common high-energy limit of 300 keV. The LoP subsystem has 10 channels with thresholds of 72, 91, 104, 125, 153, 190, 235, 292, 365, and 475 keV. The common upper energy limit is 573 keV. Although both instruments have 256 ms resolution, throughout this paper we will use 10-s spin-averaged and 1-min-averaged data. The spin axis points toward the Earth, so data averaged over one spin and all telescopes are also averaged over the unit sphere. Differential energy measurements are obtained from the nested energy measurements by subtracting adjacent channels. More information on the CPA detectors can be found in the paper by *Higbie et al.* [1978].

The two other geosynchronous spacecraft with Los Alamos instruments which were operational at that time were 1987-097, which also carried a CPA package, and 1989-046, which carried the synchronous orbit particle analyzer (SOPA). SOPA is a new generation of energetic particle analyzers. It returns data similar to those from the CPA but has somewhat different energy limits [*Belian et al.,* 1992].

The Galileo spacecraft carries a complement of field and particle instruments. In this study we have used data from the flux gate magnetometer (described in detail by *Kivelson et al.* [1992]) and the energetic particle detector (EPD) [*Williams et al.*, 1992]. The low-energy magnetospheric measurement system (LEMMS) of the Galileo energetic particle detector measures electrons and protons in the same energy range as the CPA LoE and LoP instruments. The channels of interest to this study are the A0-A5 channels, which measure protons in differential energy bins with energies of 22-42, 42-65, 65-120, 120-280, 280-515, and 515-825 keV, and the E0-E3 and F0 channels, which measure electrons in differential energy bins with energies of 15-29, 29-42, 42-55, 55-93, and 93-188 keV. In this study we use spin-averaged LEMMS data. The spin period of Galileo is approximately 20 s. In order to obtain full unit sphere coverage the EPD is also articulated with respect to the spin plane. A stepper motor moves the sensors in the plane containing the spin axis after each spin. When the particle distribution is not isotropic, this adds a modulation to the EPD data which has not been removed. Although the number of steps is controllable, during the Earth 1 flyby the modulation period is approximately 200 s.

Geosynchronous Observations

Figure 5 shows 1-min averages of the energetic electron fluxes for the three geosynchronous spacecraft between 1700 and 2100 UT. As we have seen, 1984-129 was in the midnight sector. Its longitude was 69°E. Spacecraft 1987-097 was at 8°E, so it was located near dusk, and 1989-046 was at 165°W, which put it near dawn. Local times are given at the top of each panel, and universal time is shown at the bottom of the figure. Only selected energies are plotted. For 1989-046 the plotted electron energies are 50-75, 75-105, and 105-150 keV. For 1987-097 and 1984-129 they are 30-45, 45-65, 65-95, and 95-140 keV.

The most obvious feature in these data is the dramatic series of flux dropouts and recoveries seen at spacecraft 1984-129. The first dropout began at approximately 1730 UT. A partial recovery occurred at 1759 UT, and a more complete recovery at 1811 UT. When the fluxes recovered at 1811 UT, they did not recover to their pre-event levels and, in fact, continued to decline gradually after recovery. At 1912 UT a second geosynchronous dropout began. The dropout reintensified at 1927 UT and recovered at 1941 UT. Again the recovery was not complete and showed evidence of a continued overall decline. A recovery which brought fluxes to levels above their predropout values was not seen until 2053 UT. At 2100 UT the data stream from 1984-129 was interrupted but data from the other two spacecraft (not shown) indicate a moderate-intensity dispersed injection. (This data gap and the one prior to 1930 UT for spacecraft 1987-097 occurred because the spacecraft were not tracked at those times.) During the 4-hour interval shown, the spacecraft moved 60°. Therefore the position of spacecraft 1987-097 at 2100 UT was approximately the same as the position of spacecraft 1984-129 at 1700 UT. No dropout was observed by 1987-097 either before or after 2100 UT (data not shown), so by 2100 UT the sequence of events may have been over. These flux dropouts were only observed in the midnight local time sector, as is expected for plasma sheet thinning in the substorm growth phase.

Although we saw flux recoveries at 1984-129, we did not see evidence of injections in the sense of flux enhancements. That is, the fluxes returned to their pre-event levels but did not exceed them. This observation is confirmed by the data from spacecraft 1989-046, which lay to the east of 1984-129. Any electrons injected on the appropriate drift shell near midnight would have drifted to 1989-046. Careful examination of the high time resolution electron data from 1989-046 reveals small flux changes with dispersion which is consistent with onset times of 1759, 1811, and 1844 UT, but it is clear from Figure 5 that there was no significant injection of a new population of energetic particles associated with these flux dropouts and recoveries. Although this is not typical behavior for a substorm, it is by no means uncommon [e.g., *Walker et al.,* 1978]. We also note that although there was no significant injection on the geosynchronous drift shell, these observations do not exclude the possibility of an injection on either higher or lower drift shells.

Galileo Energetic Particle Observations

Figure 6 shows several electron channels from the LEMMS detector on Galileo. The large variability in these data is also indicative of the level of disturbance of the plasma sheet during this period. From the beginning of the interval to about 1917□UT, Galileo encountered the very disturbed plasma sheet or the plasma sheet boundary layer. Spectra from the University of Iowa plasma analyzer (L. A. Frank, personal communication, 1992) confirm that Galileo did not enter the lobes during this interval. After 1917 UT, Galileo was inside geosynchronous orbit and measured the relatively undisturbed radiation belt region.

The interval plotted in Figure 6 began with Galileo measuring a burst of elevated electron fluxes which ended around 1711 UT. Fluxes remained at nearly constant or slowly decreasing levels until 1748 UT. Fluxes then dropped, rose, and dropped again before 1759 UT, when a more sustained burst of electrons was observed, particularly in the higher energies. The burst decayed with a generally ramplike signature until another burst of electrons was observed between approximately 1811 and 1820 UT. The three narrower spikes around 1830 UT last at most one or two spins and occurred periodically. These spikes are related to the stepping of the look direction of the instrument after each spin (as described in the previous section) and are the signatures of a strong directional anisotropy in the electrons.

At 1841 UT the overall characteristics of the fluxes changed abruptly. Between 1841 and 1917 UT the fluxes were highly variable and showed no steady trend. At 1917 UT the fluxes rose abruptly, and after that time a smooth radial profile of the radiation belts was observed.

Galileo Magnetometer Observations

Figure 7 shows the Galileo magnetometer measurements [*Kivelson et al.,* 1992, 1993]. The top four panels show the three components of the field (GSM coordinates) and the field magnitude from 1700 to 2000 UT. The bottom panel shows the inclination angle, □, where □=0° for a field which is entirely in the *Z*-GSM direction and □=90° for a purely radial field. After 1900 UT the field components are plotted twice on two different scales. The left-hand scale allows the variations in the tail field to be seen, while the right-hand scale is compressed by a factor of 10 so that the stronger field closer to the Earth can be plotted.

Between 1700 and 1748 UT, Galileo was near the neutral sheet and crossed it several times, as indicated by a change in sign of *Bx*. After 1748 UT, Galileo was firmly in the northern hemisphere (Bx>0) and measured strong taillike fields (□ ≈90°). From 1748 to 1811 UT the magnetic field magnitude and the Galileo electron fluxes were anticorrelated: both the broader maximums and minimums at ≈1751 and ≈1755 UT and the narrow flux peaks/field dips at 1800 and 1804 UT. Interestingly, at 1811 UT, when the geosynchronous fluxes recovered and the Galileo electrons showed another peak, there was no significant change in the field magnitude or direction. In particular, there was no rotation of the field to a more dipolelike geometry (which would be seen as a decrease in □.)

From ≈1805 to 1841 UT the field magnitude increased steadily. At 1841 UT the field strength decreased abruptly, without rotation, and from 1841 to 1917 UT the magnetic field was much more variable, showing both X and Y perturbations. After Galileo entered the radiation belt region, the magnetic field, like the particles, showed the smooth profile expected in the inner magnetosphere.

Geosynchronous and Galileo Comparisons

It is the period prior to 1920 UT, when Galileo was in the near-Earth plasma sheet, that is the subject of this paper. Specifically, how do the fluxes at Galileo compare to those at 1984-129? Figure 8 shows a comparison of fluxes measured by 1984-129 (shaded line) and Galileo (solid line) for similar energy bands. The top panel shows a comparison of electron fluxes, and the bottom panel shows a comparison of the proton fluxes. For the protons we summed three CPA energy channels to approximate a single LEMMS channel. The data are all plotted on the same scale with no offsets.

It is apparent from Figure 8 that, throughout this interval, the flux variations at Galileo and at 1984-129 were very poorly correlated. It is instructive not only to compare the geosynchronous and Galileo fluxes but also to compare the electron and proton fluxes observed by each spacecraft. Both long time scale and short time scale variations are observed, and from those we identify three intervals of primary interest.

The first event of interest is the dropout of protons and electrons seen at 1984-129 from ≈1730 to 1811 UT. The proton fluxes begin to decline somewhat earlier than the electron fluxes, due to the difference in energies rather than in particle species. This dropout event was not observed in the Galileo data. In fact, when the lowest fluxes were observed at geosynchronous orbit, enhanced electron fluxes were observed by Galileo. In contrast, the Galileo proton fluxes showed no variation during this event. Note that when the 1984-129 fluxes are at their lowest levels for this first dropout event they are nearly equal to the fluxes measured by Galileo. This is true for all energies and for both species (data not shown).

The second interval of interest to this study is the period between 1841 and 1917:30 UT when the Galileo electron and proton fluxes showed large-amplitude and frequent variations. During this period the Galileo electron and proton fluxes track each other quite closely. Particularly striking are the flux peaks at ≈1854 UT and ≈1908 UT (or, the minimums which follow them). The geosynchronous electron and proton fluxes show little variation other than a gradual decline. Galileo was inside of 10 R_E during this period, so it is of interest to know why the flux variations at the two spacecraft are so poorly correlated.

The third interval of interest is the period of closest approach of the two spacecraft. The crossover occurred at 1917:30 UT ± 30 s for all measured electron energies. The proton fluxes in Figure 8 crossed at approximately 1920 UT. Howeve r, the proton fluxes were noisier than the electron fluxes, and for protons the fluxes at different energies crossed at different times. Still, the proton fluxes at all energies (data not shown) are consistent with a crossover at 1917 UT ± 5 min. At 1917:20 UT, 1984-129 was at GSM position (-6.068, 0.049, -2.616), and at 1917:32, Galileo was at GSM position (-6.2095, 0.2347, -0.1655). Thus Galileo was at a radial distance of 6.22 R_E and 1984-129 was at 6.63 R_E. The angular separation between the two spacecraft in the GSM equatorial plane was a mere 2.5°.

The period of closest approach would be interesting in itself, but it is made more interesting by the presence of a second geosynchronous flux dropout event. At ≈1912 UT and ≈1913 UT, respectively, the Galileo and 1984-129 electron fluxes decreased sharply. The Galileo proton fluxes show a small but less significant dip. The 1984-129 proton fluxes began decreasing earlier and decreased more gradually, as was the case for the first geosynchronous dropout event. Also the 1984-129 protons fluxes apparently didn't decrease much in this dropout event. That is misleading though. The apparent shallow depth of the geosynchronous proton dropout is due to the fact that the fluxes were already near their threshold level. (The lowest geosynchronous proton fluxes plotted are at the one count per minute level, and the zero count per minute values have not been plotted.) What is remarkable is that, while 1984-129 saw the continued deepening of the dropout, after 1917:30 UT Galileo saw no evidence of it: only the smooth profile of the radiation belts.

Analysis

The First Geosynchronous Dropout

The standard interpretation of geosynchronous flux dropouts is that they result from a combination of plasma sheet thinning and radial gradients of energetic particle fluxes (as discussed earlier and illustrated in Figure 4). For a satellite located off the magnetic equator there are two main consequences of plasma sheet thinning: a rotation of the local magnetic field direction and a mapping of that field line to a different downtail distance. Is this model consistent with our observations? If the tail were in a steady state, then we could determine the radial gradient directly from the Galileo observations at different radial distances. This was not the case. Nevertheless, for both electrons and protons and for all energies, the fluxes measured by Galileo when it was outside geosynchronous orbit were consistently less than or equal to the fluxes measured by 1984-129 at geosynchronous orbit. Thus the radial gradients were present in the tail as required if the dropouts measured by 1984-129 are interpreted as the signature of mapping to a lower flux region in the tail.

What about field rotation? The geosynchronous spacecraft do not carry magnetometers, but it is possible to infer a magnetic field direction from particle data. This is done by fitting the 256-ms resolution data from all five telescopes of the CPA to a single pitch angle distribution using an optimization technique. The symmetry axis of the distribution is assumed to be the magnetic field direction. The magnitude, of course, cannot be estimated by this method. For spacecraft 1984-129, at 1700 UT, just prior to the dropout, the field was inclined 41° with respect to the Earth's rotation axis. By 1716 UT the inclination reached 44°, and by 1738 UT it increased further to 56° (based on 1-min averages of the data). We see then that the field had become more taillike which is consistent with the thinning scenario. After 1740 UT the fluxes at 1984-129 became too low to give enough statistics to determine a symmetry axis (T. E. Cayton, personal communication, 1992). However, it is likely that after 1740 UT the field became even more taillike. Likewise, we cannot say whether the field became more dipolelike at the flux recovery because the fluxes were too low and too isotropic to determine a symmetry axis.

The geosynchronous dropout events are also associated with substorm activity, as expected. Spacecraft 1984-129 was at longitude 69.17°, and at 1811 UT its nominal magnetic foot point was at 69.66° latitude. Magnetometer data from Dixon (latitude 73.55°, longitude 80.50°) and Tixie Bay (latitude 71.21°, longitude 129.00°) confirm the presence of substorm activity. From 1700 UT to approximately 2110 UT (data not shown) a sequence of small (<100 nT) magnetic bays was seen at both stations. (A larger, ≈275-nT bay began at 2110 UT at Dixon.) Evidence of substorm activity at the recovery of the first geosynchronous dropout was also found in data from the Galileo plasma wave instrument, which showed a distinct burst of auroral kilometric radiation (AKR) at 1811 UT (A. Roux, personal communication, 1992). Pi2 signatures were also seen in ground magnetograms at that time (V. Angelopoulos, personal communication, 1992). Hence we find that the geosynchronous flux dropout observations are consistent with the standard picture of a substorm-associated thinning of the plasma sheet combined with a radial gradient of energetic particle flux.

Galileo Fluxes 1700-1841 UT

From Figure 8 we see that the thinning of the inner edge of the plasma sheet which produced the dropout at geosynchronous orbit around 1730 UT did not produce a similar signature at Galileo which was 13-15 R_E downtail. The most comparable signature in the Galileo energetic particle fluxes is the decrease in proton fluxes from ≈1745 to 1841 UT. It is tempting to think that the dropout is a propagating disturbance which requires approximately 30 min to travel from geosynchronous orbit to Galileo's position, but there are several arguments against this interpretation. Geosynchronous dropouts are generally believed to be temporal phenomena: the cross-tail current intensifies gradually and is reflected in the gradual decrease of fluxes. The diversion of the current into the ionosphere, the dipolarization of the field, and the return of the fluxes are abrupt. This is not the signature of a propagating disturbance. Furthermore, bursts of AKR and Pi2s (the signatures of sudden field changes) were observed at both 1811 and 1841 UT, indicating that they are separate events. We suggest that the geosynchronous dropout represents a shorter-duration (≈30 min) and more localized reconfiguration while the flux changes seen by Galileo are signatures of a larger-scale and longer-duration change in the magnetosphere as discussed below.

The field reconfiguration that produced the dropout at geosynchronous orbit did not produce a dropout in the Galileo fluxes. However, from the magnetometer data (Figure 7) we know that Galileo was near the neutral sheet until ≈1748 UT so it is not clear that we would expect to see a dropout. After 1748 UT, Galileo was north of the neutral sheet. The elevated electron fluxes measured by Galileo between 1748 and 1811 UT were anticorrelated with the magnetic field strength. Variations in the fluxes during this interval may be due to a combination of north-south motion of the tail, which causes an apparent motion of Galileo across electron and magnetic field gradients along with variations in the intensity of the cross-tail current, which produced simultaneous changes at Galileo and at geosynchronous orbit.

When the fluxes recovered at geosynchronous orbit at 1811 UT, there was another burst of electrons at Galileo. Unlike the previous electron bursts this one was not anticorrelated with the magnetic field strength and may have been a nonadiabatic injection of particles in the plasma sheet. Not only was the magnetic field at Galileo not anticorrelated with the particle flux at 1811 UT, but it showed no perturbation at all. In particular, it showed no dipolarization of the field which would be seen as a decrease in [illegible]. This implies that if we associate the return of the geosynchronous fluxes with a dipolarization of the field then the dipolarization was limited either to radial distances or to local times that did not include Galileo's position.

It is our interpretation that the geosynchronous dropout is a perturbation on a more global and long-duration reconfiguration of the tail. Ignoring the two more dramatic dropouts seen by 1984-129 at geosynchronous orbit, we see that there is an overall decline in fluxes of nearly 2 orders of magnitude between 1700 and 2000 UT. Until 1841 UT the Galileo proton fluxes show a decline which is similar to that seen at geosynchronous orbit. If we ignore electron flux changes between 1748 and 1817 UT associated with the dropout interval, then the Galileo electrons also decline at the same rate as the geosynchronous electrons. Figure 9 shows the period from 1715 to 1845 UT in the same format as Figure 8 but with the Galileo electron fluxes multiplied by a constant factor of 700 and the Galileo proton fluxes multiplied by a factor of 200. Figure 9 shows that, with the exception of the geosynchronous dropout interval, the fluxes measured by Galileo and by 1984-129 track one another quite closely. The very different orbital motions of the two spacecraft makes it highly unlikely that 1984-129's longitudinal motion and Galileo's radial motion would produce such similar flux changes, so the changes were probably temporal.

Thus an interesting picture emerges from the comparison of the Galileo and geosynchronous fluxes during this interval. We interpret the gradual decline in fluxes seen by both spacecraft from ≈1700 to 1841 UT as evidence of a gradual reconfiguration of the entire tail field. The geosynchronous fluxes continue to decline until nearly 2100 UT (Figure 5). (The reason the Galileo fluxes do not decline after 1841 UT will be discussed in the next section.) Ignoring the shorter-term dropouts in the fluxes at 1984-129 (Figure 5), the overall decline of fluxes also looks very much like a growth phase, but, it occurs over a 4-hour period, much longer than a typical growth phase. Corroborating evidence is that the magnetic field strength measured by Galileo from ≈1800 to 1841 UT was more than twice the magnitude predicted by the Tsyganenko field model even in its most stressed configuration. [*Hammond et al.,* 1992]. Abnormally high field strength is expected during a growth phase when excess flux is loaded into the tail. Furthermore, at the end of that 4 hours (just after the data stream from 1984-129 was interrupted) an approximately 275-nT *H* bay was seen in the Dixon magnetogram, and an injection was produced at geosynchronous orbit indicating a more substantial substorm onset.

We interpret the shorter-term geosynchronous dropouts as fairly localized perturbations on the longer-term, global reconfiguration. We have shown that the first dropout is consistent with plasma sheet thinning at geosynchronous orbit but that the Galileo magnetometer and particle data show no signatures that can be interpreted as thinning and subsequent dipolarization. Therefore the geosynchronous thinning must be limited in radius or in local time. Which is the case cannot be firmly established, but some evidence points to radial localization. Tixie Bay saw the same magnetic signatures as Dixon during the dropouts. At 1811 UT, Dixon was at a local time of 2333, Tixie was at a local time of 0247, and Galileo was between the two.

A final point regarding this interval concerns the ratio of the fluxes measured at the two spacecraft. Ignoring the dropout interval, the fluxes stay in proportion to one another which, confirms the presence of a radial gradient. For electrons with energies of ≈35 keV that ratio is 700, and for protons with energies of ≈100 keV the ratio is 200. When the dropout itself is fully developed (≈1750-1811 UT), fluxes at Galileo and at geosynchronous orbit are approximately equal for both protons and electrons and for all measured energies. From the top panel of Figure 8 we see that even some of the flux variations seen by 1984-129 within the dropout appear to track with the flux variations seen by Galileo. At the time of the dropout, 1984-129 and Galileo were separated by about 2 hours in local time, so even in the unlikely event that the field line connected to 1984-129 was distorted such that it mapped to the same radial distance as Galileo, the two spacecraft probably sampled quite different places in the plasma sheet. This implies that energetic particle fluxes in the plasma sheet at distances of 13-15 R_E may have been fairly uniform during this period while the thinning which produced the geosynchronous dropout was probably quite localized. This comparison highlights the difference between the plasma sheet proper, where only small flux variations were observed, and the inner edge of the plasma sheet, where the flux variations were observed to be quite large.

Galileo Fluxes 1841-1917:30 UT

We have noted that at 1841 UT the characteristics of the fluxes measured by Galileo changed abruptly. The observation of AKR and Pi 2s (A. Roux and V. Angelopoulos, personal communication, 1992) and the Galileo magnetometer data (Figure 7) also indicate an abrupt change in the magnetic field at that time. Significantly, no dipolarization of the field (decrease in □) was seen by Galileo, and only a slight dip in the electron fluxes was seen at geosynchronous orbit. Therefore we attribute the change in Galileo particle fluxes to a field reconfiguration which moved Galileo across the trapping boundary. The trapping boundaries are different for different energies, but because of the field reconfiguration, the Galileo fluxes change at all energies simultaneously (e.g., Figure 6).

From 1841 to 1917 UT the Galileo electron and proton fluxes fluctuated between levels comparable to those measured by 1984-129 and levels over an order of magnitude lower (Figure 8). Comparison to the magnetometer data (Figure 7) again shows that the particle flux peaks occurred at times of magnetic field minimums. Therefore the particle flux variations were probably caused by field variations which moved the trapping boundary across Galileo. When the field strength decreased, the trapping region expanded, and Galileo measured fluxes similar to those measured by 1984-129. Throughout this time 1984-129 remained within the trapping region and measured little variation of flux other than the gradual decrease discussed above.

The fact that Galileo moved in and out of the trapping region at such a wide range of radial distances means either that Galileo was skimming the trapping boundary or that the trapping region was changing its size by several Earth radii in a matter of minutes. Figure 10 shows that the former is more plausible. Figure 10 is an enlargement of Figure 3, which shows the Galileo trajectory after 1847 UT along with the field lines predicted in the Tsyganenko model. We see that if the magnetic field were even more taillike than in the most stretched Tsyganenko model then the Galileo trajectory would be nearly parallel to the field. Galileo magnetometer observations confirm that the field was inclined to be nearly parallel to the spacecraft trajectory. Therefore relatively small north-south motions of the trapping region could cause the flux variations seen by Galileo. IMP 8 solar wind observations indeed show that the solar wind was highly variable throughout the interval studied here [*Saunders et al.,* 1992; *Kivelson et al.,* 1993]. After 1917:30 UT, Galileo was inside geosynchronous orbit and did not encounter the trapping boundary again.

Closest Approach

At 1917:30 UT the fluxes of electrons measured by Galileo and by 1984-129 were equal (Figure 8). Since Galileo measured increasing fluxes and 1984-129 measured decreasing fluxes one might think that this time was simply coincidental. But the fact that the fluxes crossed at the same time in six energy channels from ≈30 to ≈300 keV gives us confidence that the two spacecraft were, in fact, on the same drift shell at that time. (The proton fluxes are consistent with this conclusion but have a greater uncertainty, as discussed above.)

This crossing time supports the conclusion that the magnetic field at geosynchronous orbit was quite distorted. From Figure 10 we see that Galileo was at a radial distance of 6.22 R_E at 1917:30 UT and that, according to the Tsyganenko model, Galileo should have crossed the geosynchronous drift shell several minutes earlier. However, if, as we argued in the previous section, the trapping boundary (and hence the field lines) was distorted such that Galileo's trajectory was nearly parallel to it, then it is quite believable that the point at which the fluxes were equal is the point at which the two spacecraft were on the same drift shell.

The closest approach is interesting not only for its geometry but also for its dynamics. At ≈1912 and ≈1913 UT, respectively, the electron fluxes measured by Galileo and by 1984-129 decreased as a change in the magnetic field moved the trapping boundary across both spacecraft. As the field became more distorted and the inner plasma sheet became thinner, 1984-129 became magnetically connected to the lower fluxes of the more distant plasma sheet again. In contrast, the Galileo fluxes increased. The dropout of fluxes measured by 1984-129 is a temporal effect, while the increase of fluxes measured by Galileo is clearly the effect of crossing a spatial boundary. As soon as Galileo crossed the geosynchronous drift shell, it measured fluxes which were approximately equal to the fluxes measured by 1984-129 before the dropout. Therefore Galileo entered a region which was affected by the large-scale, long-duration flux decreases but was unaffected by the localized processes which produced the two more dramatic geosynchronous dropouts.

Although we can again identify the geosynchronous dropouts as time-dependent but spatially localized phenomena, there is again ambiguity as to the nature of this localization. The dropout region could have been localized in radius, in azimuth, or in latitude. If the dropout region was limited only in radius, then it must have had a rather sharp inner boundary. We have concluded that at 1917:30 when Galileo was at 6.2 R_E it was on the same magnetic shell as the geosynchronous spacecraft 1984-129. Just after that time, though, 1984-129 was in the dropout region but Galileo was not. Therefore at Galileo's magnetic latitude the sharp boundary would have had to be in the vicinity of 6.2 R_E.

Since the spacecraft were separated in local time by only 2.5°, an azimuthal dependence alone would also imply an extremely sharp boundary. The different latitudes (northern and southern hemispheres) of the two spacecraft relaxes these conditions somewhat. Even though Galileo was quite close to local midnight, there was a reasonably strong Y component to the magnetic field (Figure 7). The magnetic shear implied could make the effective azimuthal separation of the two spacecraft somewhat larger. In addition, the substantial deviation of the field from its nominal shape makes the difference in effective radius between the two spacecraft more ambiguous.

Finally, it is interesting to note that the long-duration changes, which we have argued are more global, appear to affect even the region well inside geosynchronous orbit. From Figure 8 we see that the fluxes measured by Galileo at the peak of the radiation belts (≈1945 UT) are actually lower than the fluxes measured at geosynchronous orbit at 1700 UT, prior to the long flux decrease.

Conclusions

We have examined energetic particle data during the Galileo Earth□ flyby on December 8, 1990. Between 1700 and 2

000 UT, Galileo's trajectory made a radial cut through the near-Earth plasma sheet in the midnight sector, while the geosynchronous spacecraft 1984-129 made an azimuthal pass through the same region. During this period a series of energetic particle dropouts were observed. The first of these began at approximately 1730 UT and lasted approximately 40 min. The last observed dropout event ended just prior to 2100 UT.

Our analysis supports the association of geosynchronous flux dropouts with the thinning of the near-Earth plasma sheet. The dropouts occurred in the midnight local time sector during a period of weak substorm activity. Both protons and electrons of all measured energies were affected simultaneously, consistent with the interpretation that the dropouts are caused by a magnetic field reconfiguration. An analysis of the symmetry axis of the geosynchronous electron distribution also confirms a rotation of the field direction toward a more taillike geometry at the beginning of the first dropout event. We suggest that as the field became more distorted the trapping boundary moved across the geosynchronous spacecraft, which became magnetically connected to the more distant plasma sheet. A comparison of the levels of energetic electron and proton fluxes at Galileo shows that the fluxes were consistently lower tailward of geosynchronous orbit, confirming the expected particle flux gradient.

We also found, though, that the reconfiguration of the tail occurred on two separate spatial and temporal scales. The geosynchronous dropouts which are commonly associated with the growth phase of substorms occurred during periods of only weak ground auroral magnetic activity. They also appear to be quite localized in azimuth and/or radius. During the first geosynchronous dropout, Galileo at 13-15 R_E observed only an apparent motion of the tail which varied the magnetic field strength and the energetic electron fluxes. At 1811 UT the fluxes recovered at geosynchronous orbit. Such abrupt recoveries are typically associated with substorm onset. The observation of AKR and Pi2s also indicates an impulsive change in the magnetic field, but no impulsive field change (such as dipolarization of the field) was observed by Galileo. Hence the changes in the plasma sheet proper appear to be much less dramatic than those at geosynchronous orbit during this dropout.

During the second geosynchronous dropout, Galileo and 1984-129 were in remarkably close proximity. Nevertheless, as the dropout intensified at the location of 1984-129, Galileo moved into an undisturbed part of the geosynchronous region. Although the distortion of the magnetic field and the longitudinal separation of the two spacecraft relax the constraints on spatial localization somewhat, the fact that the spacecraft were separated by 0.4 R_E and 2.5° azimuth at closest approach still argues for a high degree of spatial structure. Although a high degree of spatial structure has been observed in the more distant tail [e.g., *Kivelson et al.,* 1993; *Lin et al.,* 1991] and in the injection of particles at substorm onset [e.g., *Lopez et al.,* 1988; *Reeves et al.,* 1992], this is, to our knowledge, the first report of such localization for substorm dropouts at geosynchronous orbit. This result does not appear to be consistent with the common belief that dropouts are caused by the intensification of a large-scale cross-tail current.

The feature in our data which would be more consistent with the expected signature of intensification of the cross-tail current is the gradual decrease of fluxes over the 4-hour interval from ≈1700 to ≈2100 UT. Although this is much longer than the time scale for a typical substorm growth phase, some of our observations support that interpretation. The long term flux decrease was more global than the geosynchronous dropouts. Between 1715 and 1841 UT (with the exception of the dropout itself) the fluxes at Galileo decrease at the same rate as the fluxes at geosynchronous orbit. During that same time the magnetic field strength in the plasma sheet was more than double its expected value indicating excess flux in the tail. Also, shortly after 2100 UT, there was an injection at geosynchronous orbit and the Dixon magnetometer recorded the onset of a moderate substorm bay. The geosynchronous dropouts appear to be perturbations on this unusually long "growth phase." They are more local, they are not followed by substorm injections, and they are associated only with very weak ground magnetic signatures.

We were also able to identify the spatial regions sampled by the Galileo spacecraft and to distinguish spatial variations from temporal changes. From 1700 to 1841 UT, Galileo measured gradually decreasing fluxes in the plasma sheet. We have identified this as a temporal change affecting the entire tail. The bursts of electrons seen by Galileo during the geosynchronous dropout are anticorrelated with the magnetic field intensity and appear to be caused by a north-south motion of the magnetotail. The exception was the small burst of electrons seen by Galileo at the time of the geosynchronous recovery, which was not accompanied by a change in the magnetic field.

During the first geosynchronous dropout the fluxes measured by Galileo and by 1984-129 were nearly equal. It is highly unlikely that the two spacecraft were magnetically connected. This may indicate that the plasma sheet in the region of 13-15 R_E contained relatively spatially uniform fluxes of energetic particles during this interval.

At 1841 UT there was a second impulsive change in the magnetic field accompanied by AKR and Pi2s. This time Galileo observed the effects, but 1918-129 was affected very little. The reorganization of the field abruptly changed the size of the trapping boundary, and Galileo became immersed in it. The variations in particle flux seen by Galileo after that suggest that the trapping boundary was shaped such that Galileo's trajectory was nearly parallel to it. This implies a substantial distortion of the magnetic field in the vicinity of geosynchronous orbit into a much more taillike configuration than that predicted by standard models. This is consistent both with previous studies [e.g., *Kaufmann,* 1987] and with our observation of the location of Galileo when it crossed the geosynchronous drift shell. The final transition from the trapping boundary region into the stable trapping region occurred, not because of a change in the magnetic field, but because of the orbital motion of the spacecraft. In fact, the observations of 1984-129 show that the magnetic field was chan ging in such a way as to move Galileo out of the trapping region.

The fortuitous configuration of spacecraft during the Galileo Earth❑1 flyby highlights the value of multispacecraft studies of the magnetosphere for resolving temporal and spatial phenomena. It also reinforces the view that magnetospheric substorms can be not only quite complex, but also quite varied in their manifestation.

Acknowledgments. This work was supported by the Department of Energy Office of Basic Energy Sciences. Work at UCLA was partially supported by the Jet Propulsion Laboratory under contract JPL-958694. The authors would like to thank Kristen Parker and Ken Heres for their invaluable assistance in processing the Galileo EPD data. We would also like to thank Vassilis Angelopoulos for magnetic pulsation data, Alan Roux for Galileo plasma wave data, Lou Frank for Galileo plasma data, Tom Cayton and Karla Sofaly for determination of the magnetic field direction from geosynchronous particle data, and numerous participants in the Galileo Earth□ Workshop for lively and valuable discussions.

The Editor thanks A. L. Vampola and B. A. Whalen for their assistance in evaluating this paper.

References

Arnoldy, R. L., and K. W. Chan, Particle substorms observed at the geostationary orbit, *J. Geophys. Res., 74,* 5019, 1969.

Baker, D. N., and R. L. McPherron, Extreme energetic particle decreases near geostationary orbit: A manifestation of current diversion within the inner plasma sheet, *Adv. Space Res., 10,* 131, 1990.

Baker, D. N., R. D. Belian, P. R. Higbie, and E. W. Hones, Jr., High-energy magnetospheric protons and their dependence on geomagnetic and interplanetary conditions, *J. Geophys. Res., 84*, 7138, 1979.

Baker, D. N., E. W. Hones, P. R. Higbie, R. D. Belian, and P. Stauning, Global properties of the magnetosphere during a substorm growth phase: A case study, *J. Geophys. Res., 86,* 8941, 1981.

Belian, R. D., D. N. Baker, E. W. Hones, Jr., P. R. Higbie, S. J. Bame, and J. R. Asbridge, Timing of energetic proton enhancements relative to magnetospheric substorm activity and its implication for substorm theories, *J. Geophys. Res., 86*, 1415, 1981.

Belian, R. D., G. R. Gisler, T. Cayton, and R. Christensen, High Z energetic particles at geosynchronous orbit during the great solar proton event of October, 1989, *J. Geophys. Res., 97,* 16,897, 1992.

Bogott, F. H., and F. S. Moser, Drifting energetic particle bunches observed on ATS 5, *J. Geophys. Res., 79,* 1825, 1974.

Hammond, C. M., M. G. Kivelson, and R. J. Walker, Translunar observations of tail flux during the Galileo Earth 1 encounter, *EOS Trans. AGU 73(43)*, 471, 1992.

Higbie, P. R., R. D. Belian, and D. N. Baker, High-resolution energetic particle measurements at 6.6 R_E, 1, Electron micropulsations, *J. Geophys. Res., 83,* 4851, 1978.

Hones, E. W., J. R. Asbridge, S. J. Bame, and I. B. Strong, Outward flow of plasma in the magnetotail following geomagnetic bays, *J. Geophys. Res., 72*, 5879, 1967.

Hones, E. W., J. R. Asbridge, S. J. Bame, and S. Singer, Substorm variations of the magnetotail plasma sheet from $X\text{-}sm \approx -6\ R_E$ to $X\text{-}sm \approx 60\ R_E$, *J. Geophys. Res., 78*, 109, 1973.

Kaufmann, R. L., Substorm currents: Growth phase and onset, *J. Geophys. Res., 92,* 7471-7486, 1987.

Kivelson, M. G., K. K. Khurana, J. D. Means, C. T. Russell, and R. C. Snare, The Galileo magnetic field investigation, *Space Sci. Rev., 60,* 357, 1992.

Kivelson, M. G., et al., The Galileo Earth encounter: Magnetometer and allied measurements, *J. Geophys. Res., 98,* 11,299, 1993.

Lezniak, T. W., and J. R. Winckler, Experimental study of magnetospheric motions and the acceleration of energetic electrons during substorms, *J. Geophys. Res., 75*, 7075, 1970.

Lin, N., R. L. McPherron, M. G. Kivelson, and R. J. Walker, Multipoint reconnection in the near-Earth magnetotail: CDAW 6 observations of energetic particles and magnetic field, *J. Geophys. Res., 96,* 19,427, 1991.

Lopez, R. E., D. N. Baker, A. T. Y. Lui, D. G. Sibeck, R. D. Belian, R. W. McEntire, T. A. Potemra, and S. M. Krimigis, The radial and longitudinal propagation characteristics of substorm injections, *Adv. Space. Res., 8*, 91, 1988.

Lopez, R. E., A. T. Y. Lui, D. G. Sibeck, K. Takahashi, R. W. McEntire, L. J. Zanetti, and S. M. Krimigis, On the relationship between energetic particle flux morphology and the change in the magnetic field magnitude during substorms, *J. Geophys. Res., 94*, 17,105, 1989.

Lopez, R. E., R. W. McEntire, T. A. Potemra, D. N. Baker, and R. D. Belian, A possible case of radially antisunward propagating substorm onset in the near-Earth magnetotail, *Planet. Space Sci., 38*, 771, 1990.

Lui, A. T. Y., A synthesis of magnetospheric substorm models, *J. Geophys. Res., 96*, 1849, 1991.

McIlwain, C. E., Substorm injection boundaries, in *Magnetospheric Physics*, edited by B. M. McCormac, p. 143, D. Reidel, Hingham, Mass., 1974.

Reeves, G. D., R. D. Belian, and T. A. Fritz, Numerical tracing of energetic particle drifts in a model magnetosphere, *J. Geophys. Res., 96*, 13,997, 1991.

Reeves, G. D., G. Kettmann, T. A. Fritz, and R. D. Belian, Further investigation of the CDAW 7 substorm using geosynchronous particle data: Multiple injections and their implications, *J. Geophys. Res., 97*, 6417, 1992.

Saunders, M. A., M. P. Freeman, D. J. Southwood, S. W. H. Cowley, M. Lockwood, J. C. Samson, C. J. Farrugia, and T. J. Hughes, Dayside ionospheric convection changes in response to long period IMF oscillations: Determination of the ionospheric phase velocity, *J. Geophys. Res., 97,* 19,373, 1993.

Sauvaud, J. A., and J. R. Winckler, Dynamics of plasma, energetic particles, and fields near synchronous orbit in the nighttime sector during magnetospheric substorms, *J. Geophys. Res., 85*, 2043, 1980.

Tsyganenko, N. A., A magnetospheric magnetic field model with a warped tail current sheet, *Planet. Space Sci, 37,* 5, 1989.

Walker, R. J., K. N. Erickson, and J. R. Winckler, Pitch angle dispersion of drifting energetic protons at synchronous orbit, *J. Geophys. Res., 83*, 1595, 1978.

Williams, D. J., R. W. McEntire, S. Jaskuler, and B. Wilken, The Galileo energetic particle detector, *Space Sci. Rev., 60,* 385, 1992.

R. D. Belian, T. A. Fritz, and G. D. Reeves, Los Alamos National laboratory, SST-9, MS D-436, Los Alamos, NM 87545.

M. G. Kivelson, University of California, Los Angeles, CA 90024.

R. W. McEntire, E. C. Roelof, and D. J. Williams, The Johns Hopkins University Applied Physics Laboratory, Laurel, MD 20723.

B. Wilken, Max-Planck-Institut für Aeronomie, Postfach 20, D-3411 Katlenburg-Lindau, Germany

(Received March 2, 1993;
revised June 30, 1993;
accepted August 6, 1993.)

[1] Los Alamos National Laboratory, Los Alamos, New Mexico.

[2] The Johns Hopkins University Applied Physics Laboratory, Laurel, Maryland.

[3] University of California, Los Angeles, California.

[4] Max-Planck-Institut für Aeronomie, Katlenburg-Lindau, Germany.

Paper number 93JA02290.
0148-0227/93/93JA-02290 $05.00

Figure Captions

Fig. 1. The Galileo Earth□ Flyby trajectory in the *GSE X-Y* and *X-Z* planes. Dots are plotted on top of the trajectory curve for each hour from 0100 to 2400 UT.

Fig. 2. The trajectories of Galileo and geosynchronous spacecraft 1984-129. Positions are marked for each hour from 1700 to 2000 UT. Galileo made a nearly radial pass through the midnight sector while 1984-129 made an azimuthal pass. At approximately 1917:30 UT, Galileo crossed the geosynchronous orbit within 2.5° longitude of the position of 1984-129.

Fig. 3. The Galileo trajectory plotted as a function of Z-GSM and radius $(X^2+Y^2+Z^2)^{1/2}$. In this coordinate system 1984-129 is nearly motionless over this 3-hour period. Also shown are the magnetic field lines connected to 1984-129 as predicted by the *Tsyganenko* [1989] model for conditions of *Kp*=0 (quiet), *Kp*=2 (moderate), and *Kp*>4+ (disturbed) geomagnetic conditions. Although 1984-129 was in the southern hemisphere and Galileo was in the northern hemisphere, they were at nearly conjugate magnetic latitudes.

Fig. 4. A schematic of the relationship between plasma sheet thinning and energetic particle dropouts. Three field lines connected to the spacecraft at times of various amounts of plasma sheet thinning are shown. Thinning of the plasma sheet produces a local rotation of the field measured by a satellite off the equator and a mapping of the field line passing through the satellite to a location further downtail. When an earthward gradient of energetic particle fluxes exists, the change in

mapping produces a decrease in the measured energetic particle fluxes.

Fig. 5. Selected energy channels from the three geosynchronous spacecraft 1989-046, 1987-097, and 1984-129. The energies which are plotted and the spacecraft IDs are in the upper right corner of each plot. Local time is shown above each plot, and universal time is shown across the bottom. Spacecraft 1984-129 observed a series of flux dropouts and recoveries as it passed through the midnight sector. Relatively little activity was observed by 1987-097, which was in the premidnight sector, or by 1989-046, which was in the morning sector, where any injected electrons would be expected to be seen.

Fig. 6. The Galileo LEMMS electron fluxes for 1700-2000 UT. Highly variable fluxes were measured prior to 1917 UT as Galileo observed both spatial and temporal variations. After 1917 UT Galileo was inside geosynchronous orbit passing through the radiation belts, and smooth flux profiles were observed.

Fig. 7. Data from the UCLA magnetometer on Galileo . All three components of the magnetic field, its magnitude, and the colatitude angle of the field (□) are shown. After 1900 UT the data are plotted on a second, compressed scale given to the right. The two scales allow both small- and large-amplitude variations to be seen.

Fig. 8. A comparison of geosynchronous (shaded line) and Galileo (solid line) fluxes. Electrons are shown in the top panel and protons are shown in the bottom panel. For electrons the Galileo LEMMS and 1984-129 CPA instruments had very similar energy bands, so a direct flux comparison can be made. For protons, three energy bands from the 1984-129 CPA instrument have been added together to show the flux from 72-125 keV which can be compared with the Galileo LEMMS fluxes from 65 to 120 keV. Galileo crossed the geosynchronous drift shell at 1917:30 UT when the electron fluxes measured by the two spacecraft were equal.

Fig. 9. A comparison of geosynchronous and Galileo fluxes from 1715 to 1845 UT in the same format as Figure 8. The Galileo electron fluxes have been multiplied by a factor of 700, and the proton fluxes by a factor of 200. With the exception of the geosynchronous dropout interval, the Galileo fluxes decrease at the same rate as the geosynchronous fluxes.

Fig. 10. An enlargement of Figure 3 showing the period of closest approach and the field lines predicted by the Tsyganenko model. At 1917:30 UT when the fluxes at Galileo and 1984-129 were equal, Galileo was slightly inside 6.6 R_E and equatorward of the conjugate point to 1984-129 (defined as the point where the three field lines intersect in the northern hemisphere).

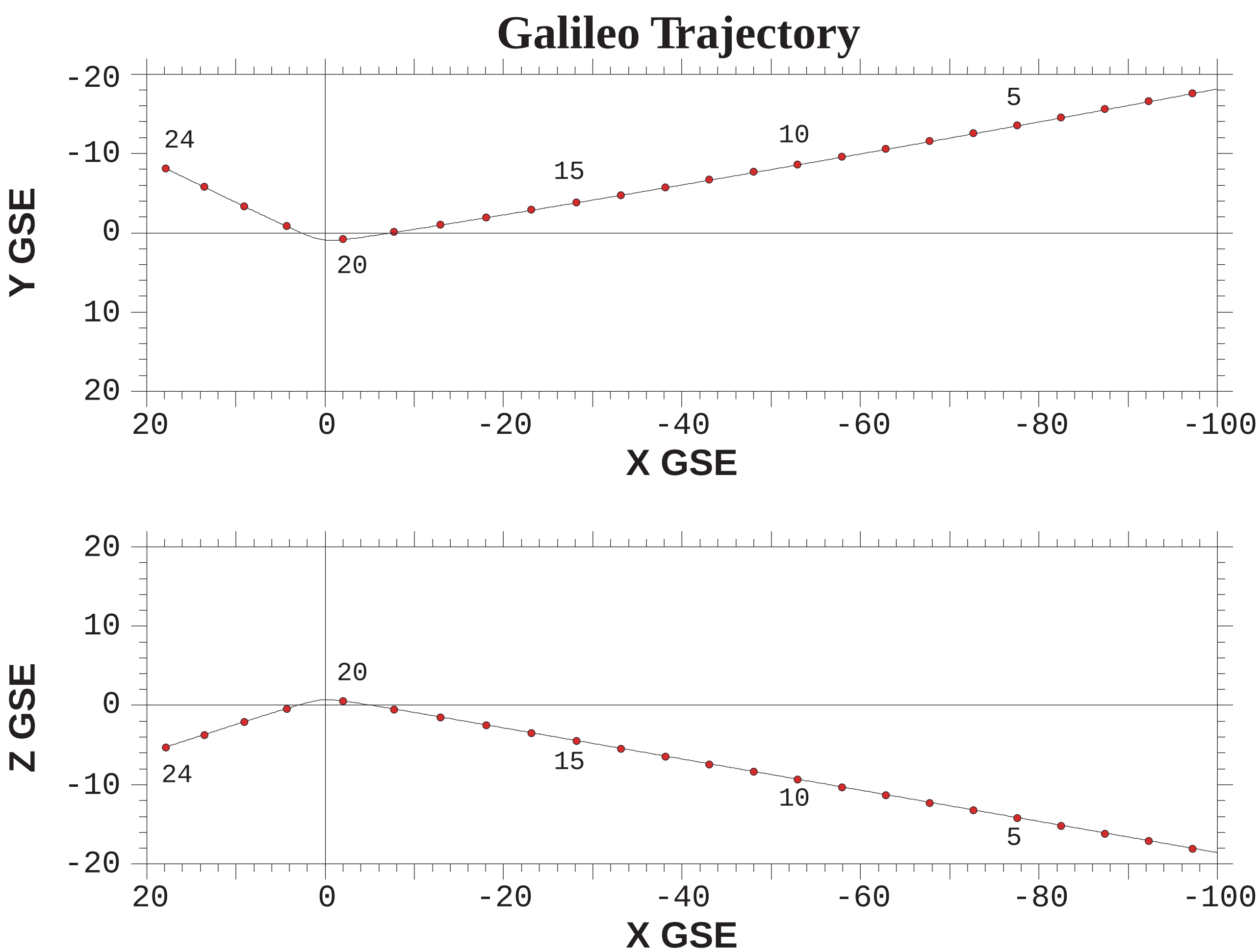

Reeves et al.,
JGR 1993
figure 1

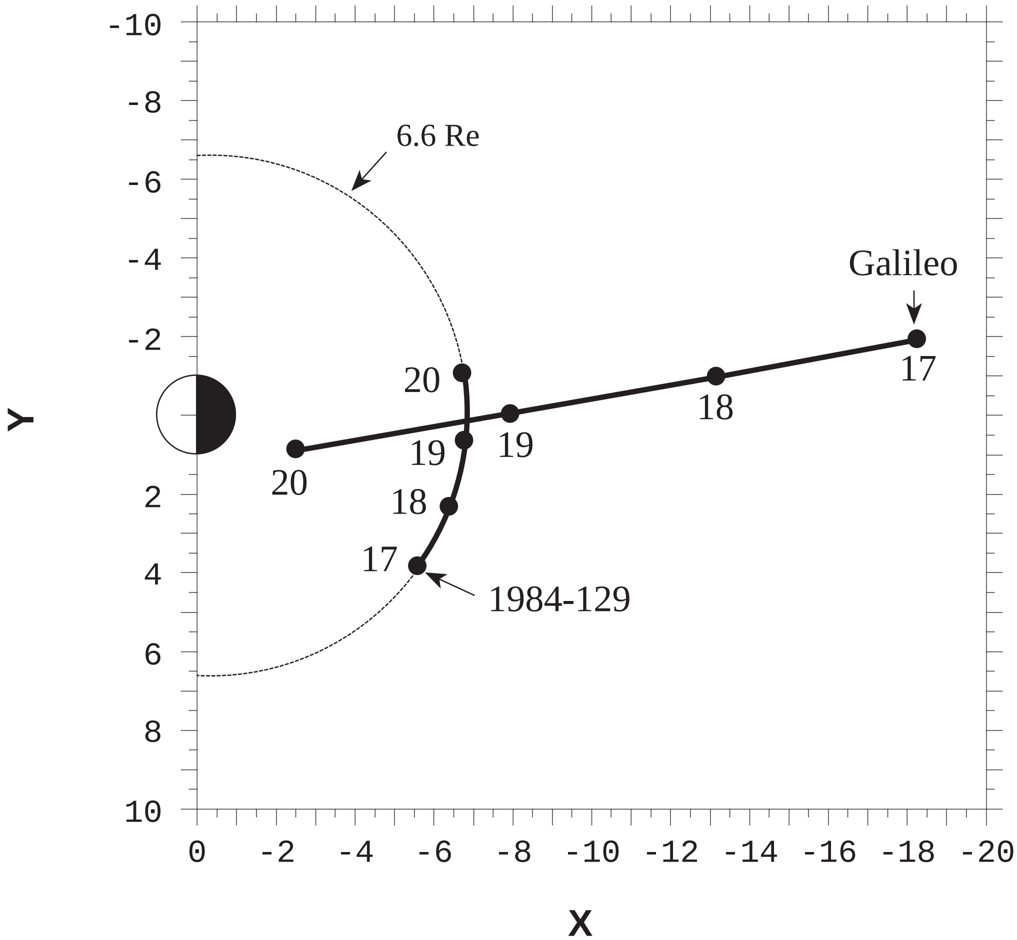

Reeves et al.,
JGR 1993
figure 2

Figur
e 2

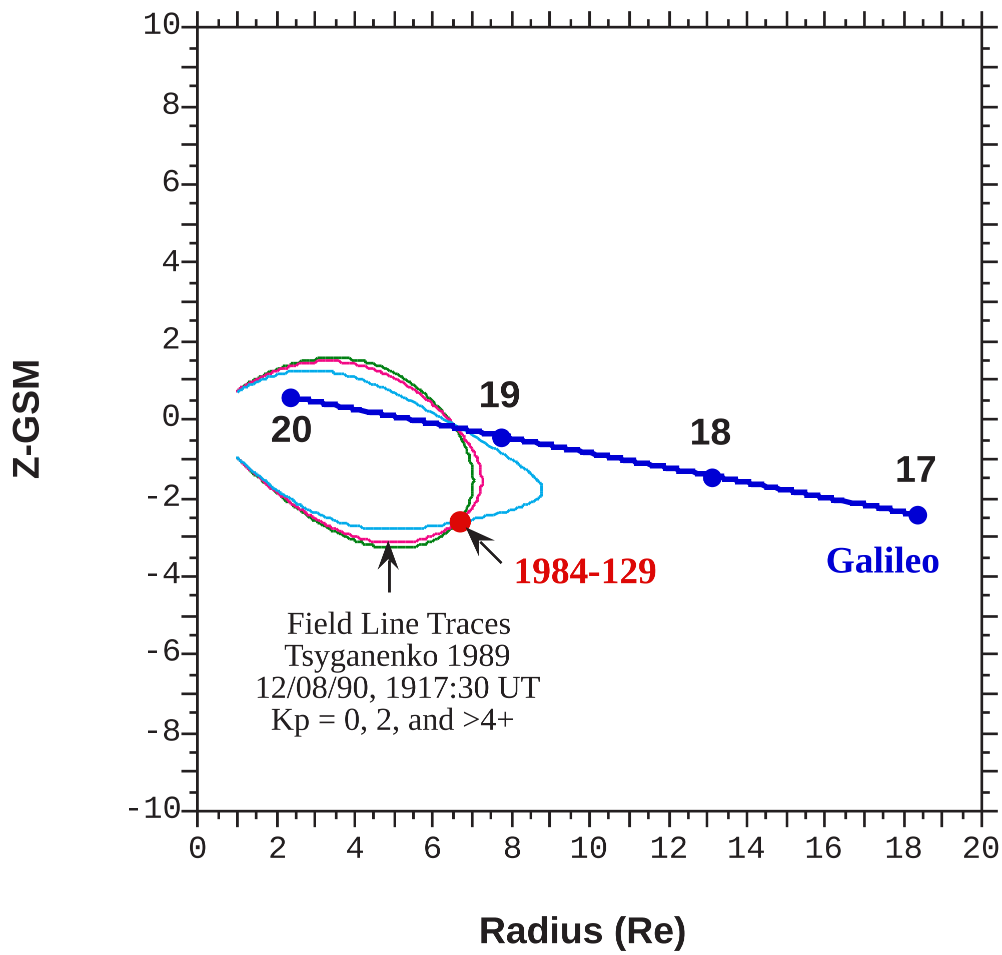

Z-GSM
10
8
6
4
2
0
-2
-4
-6
-8
-10
0
2
4
6
8
10
12
14
16
18
20
Radius (Re)
20
19
18
17
Galileo
1984-129
Field Line Traces
Tsyganenko 1989
12/08/90, 1917:30 UT
Kp = 0, 2, and >4+

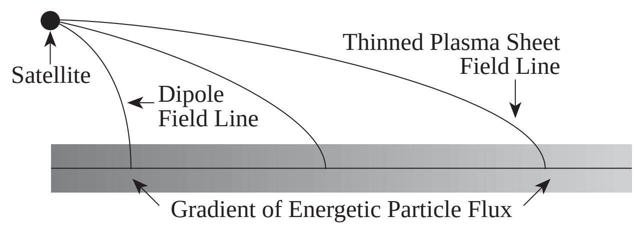

Reeves et al.,
JGR 1993
figure 4

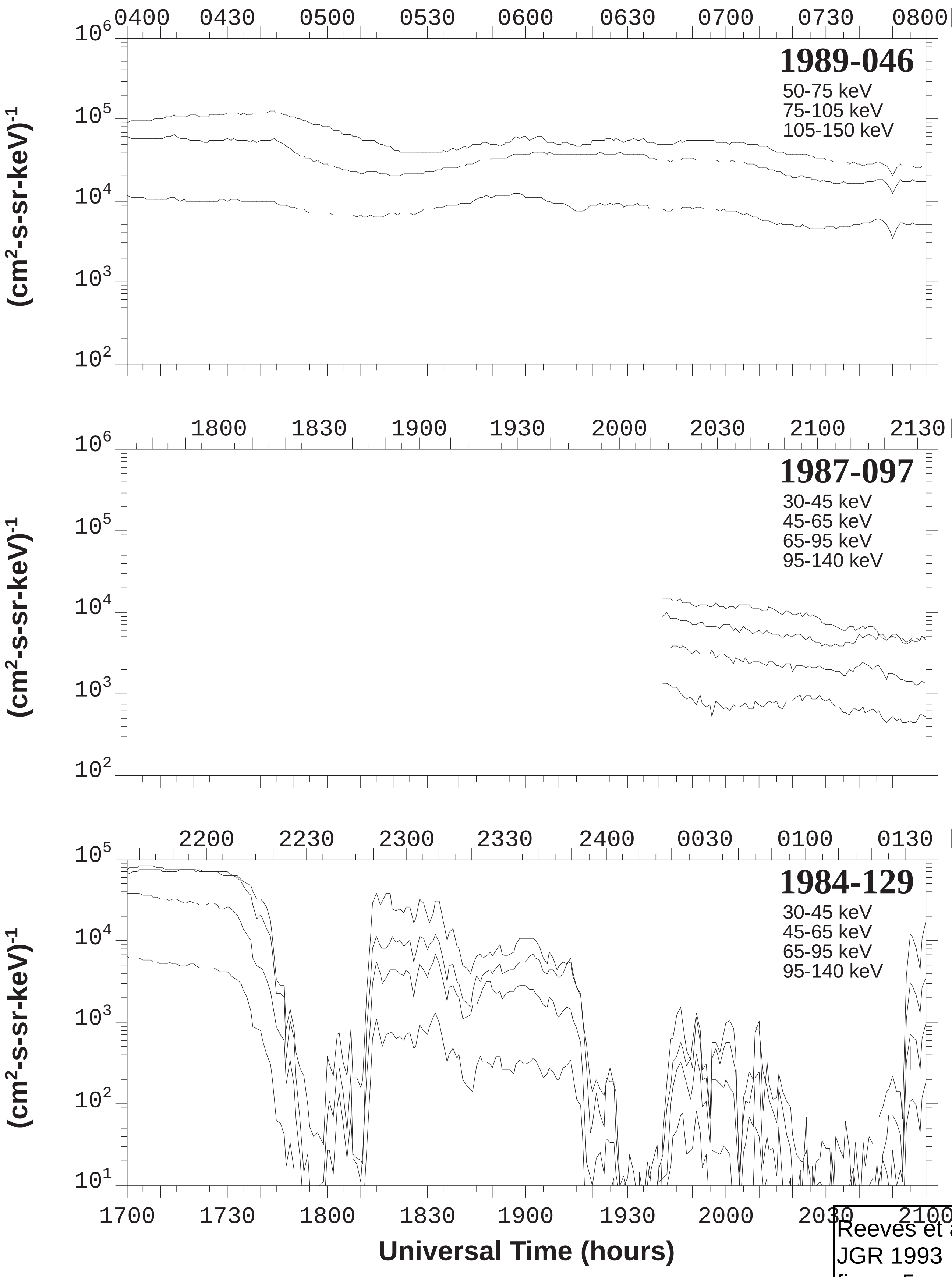

Reeves et al., JGR 1993 figure 5

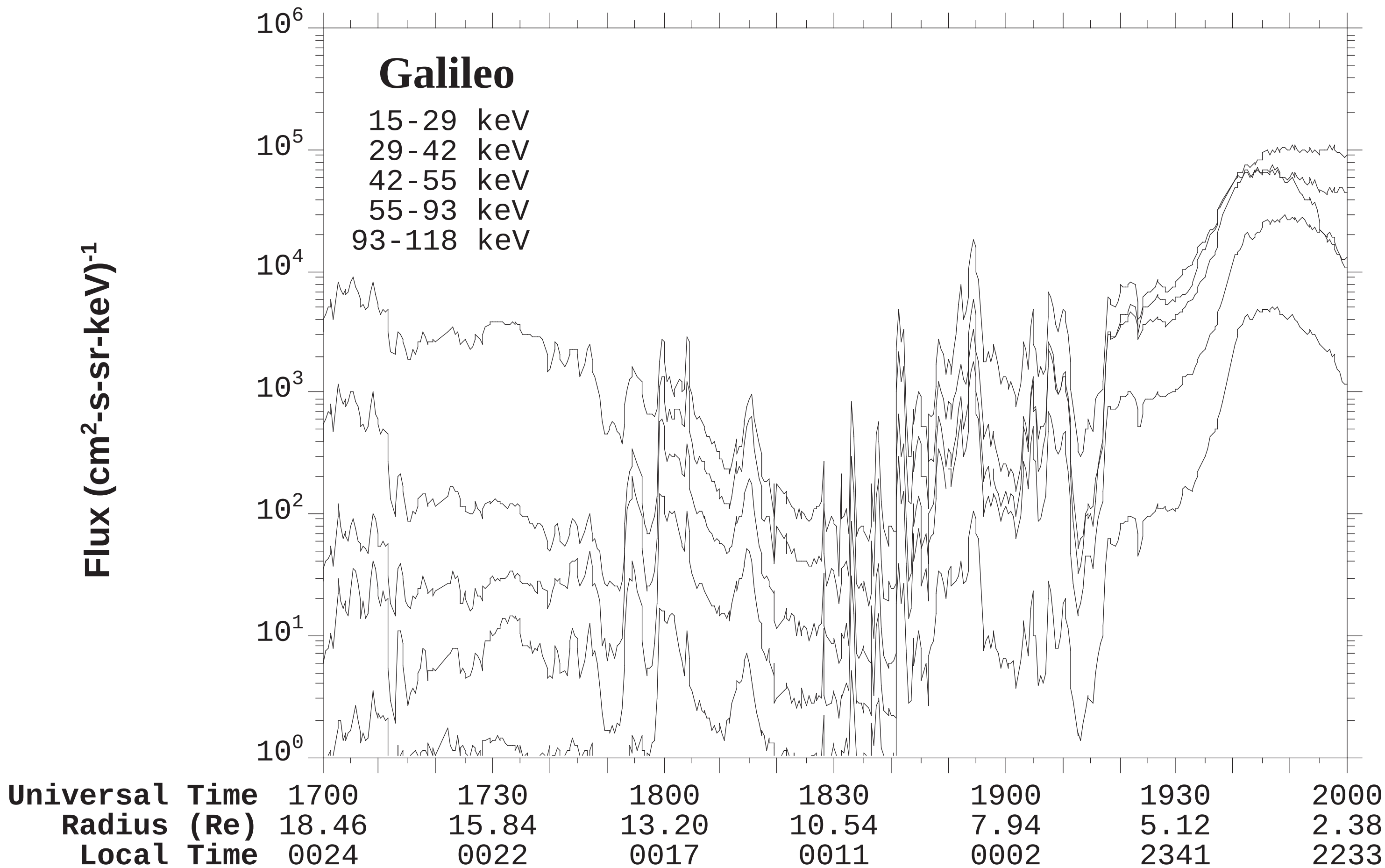

Reeves et al.,
JGR 1993
figure 6

Figure 7 not available electronically

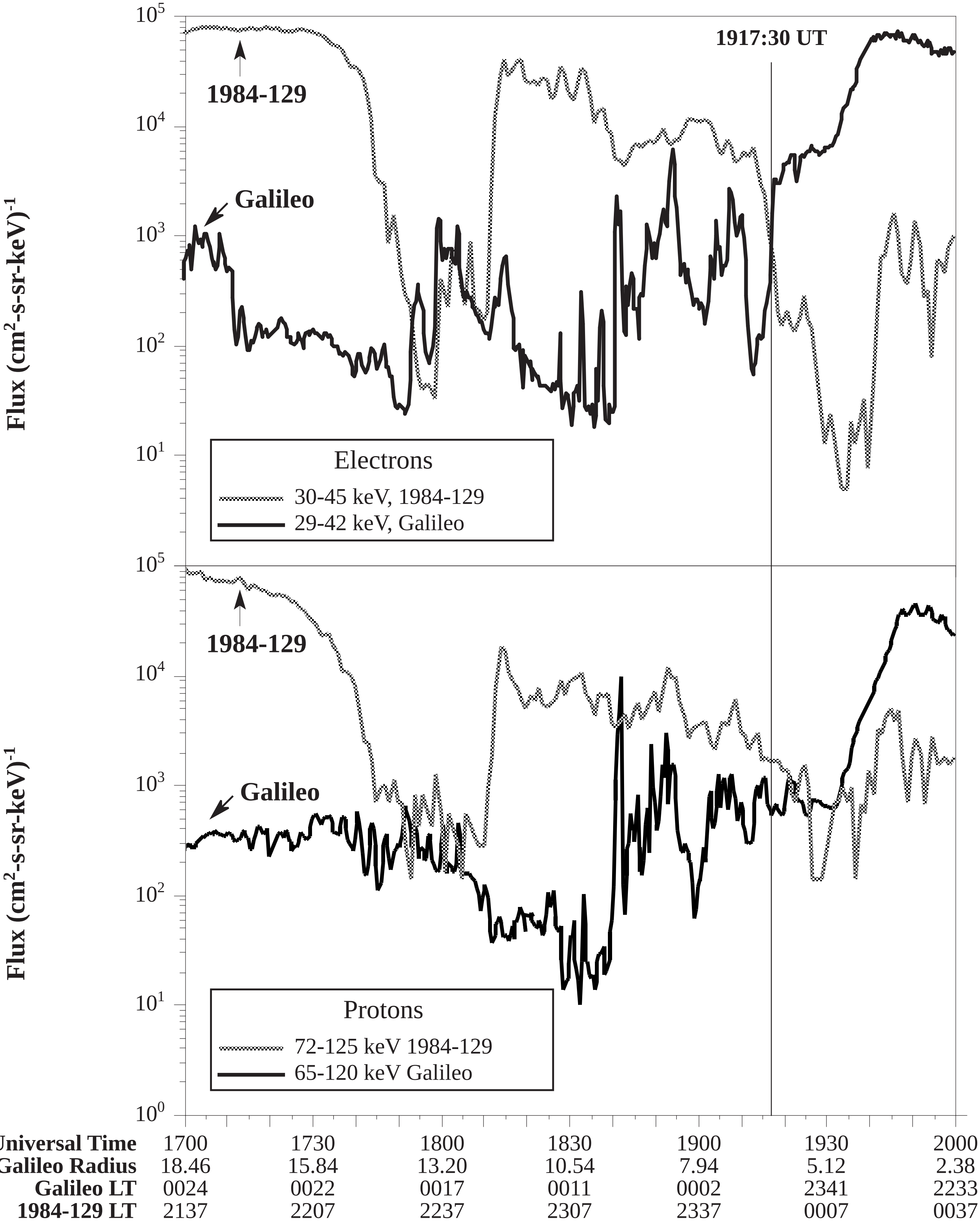

Reeves et al.,
JGR 1993
figure 8

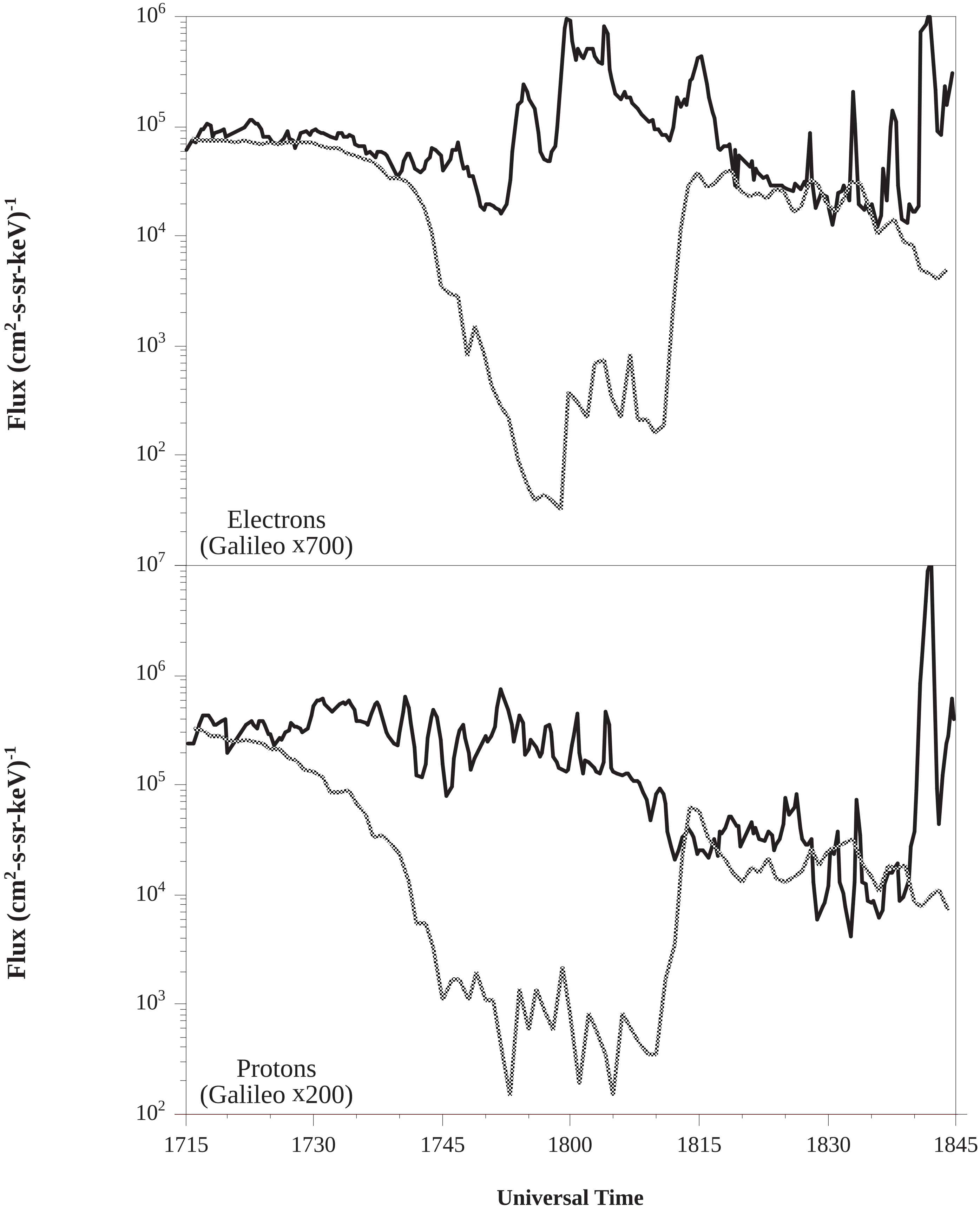

Reeves et al.,
JGR 1993
figure 9

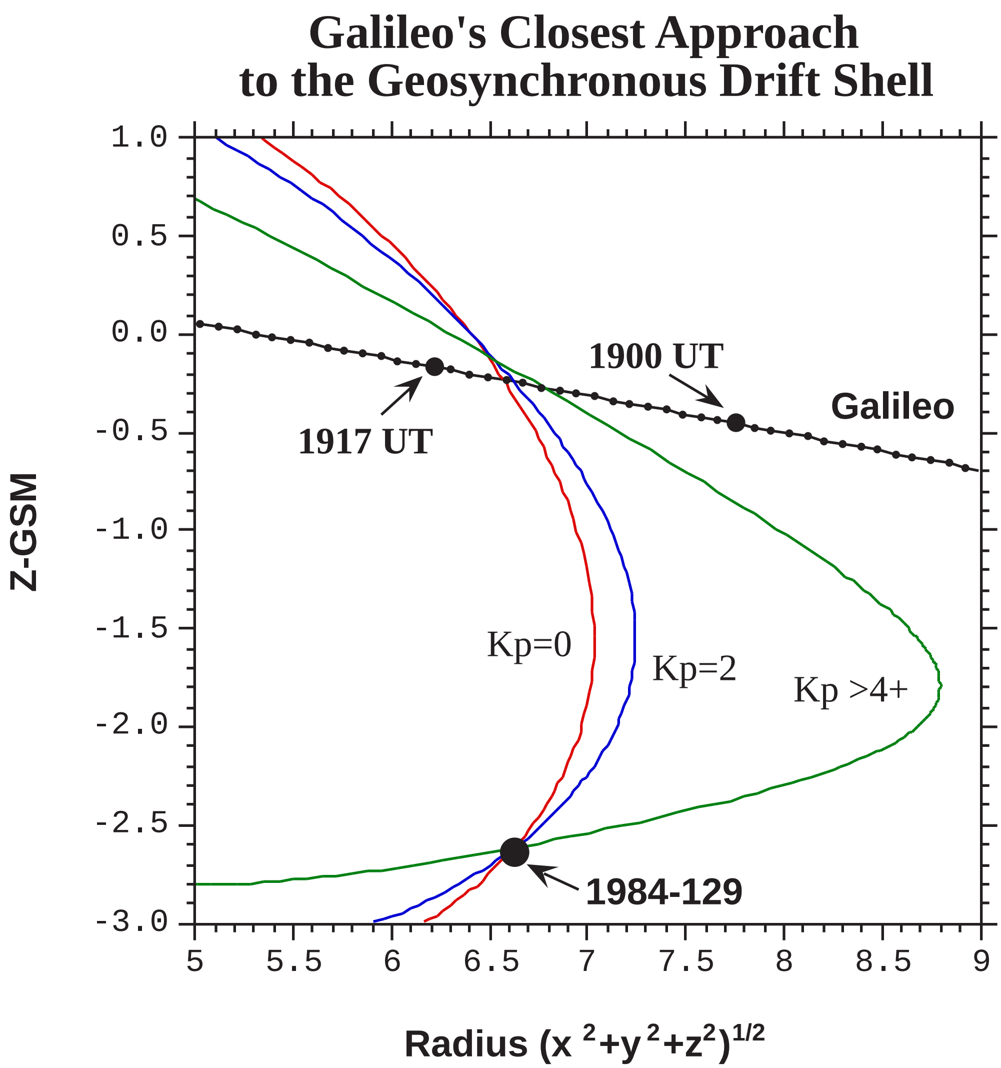

Reeves et al.,
JGR 1993
figure 10